JMEPEG (2001) 10:456–459

Mechanical Properties of 32Mn-7Cr-0.6Mo-0.3N Austenitic Steel for Cryogenic Applications

Fu Ruidong, Zheng Yangzeng, and Ren Yibin

(Submitted 26 January 2001; in revised form 18 April 2001)

The tensile, impact, and fracture toughness tests from ambient temperature to 77 K were carried out on 32Mn-7Cr-0.6Mo-0.3N austenitic steel. The fracture surfaces and the phase constitution were analyzed using scanning electron microscopy and x-ray diffraction. The results show that the relation between yield strength and temperature is $\sigma_{0.2} \cdot 300 + 1392.4 \exp(-0.0106T)$. The 77 K yield strength is 883 MPa $\cdot$ $m^{1/2}$ and the $K_{J0.05}$ value is about 236 MPa $\cdot$ $m^{1/2}$. The cryogenic intergranular fracture is fully suppressed. The 77 K fracture surfaces exhibit a tough character composed of many dimples and few small quasi-cleavage facets. The results of x-ray analysis show that the austenite phase of the steel is stable even under cryogenic deformation conditions.

Keywords cryogenic property, high manganese austenitic steel

1. Introduction

With the requirement for the cryogenic properties of the structural materials used in construction of superconducting equipment and other cryogenic engineering equipment being higher and higher, the traditional 300 austenitic stainless steels are not satisfactory for the requirement. Nickel decreases the solubility of nitrogen in steels, whereas manganese and chromium increase it. Thus, compared with Cr-Ni austenitic steels, Cr-Mn austenitic steels have higher nitrogen strengthening capability. However, high manganese austenitic steels have a tendency of cryogenic intergranular fracture (IGF),[1,2] which prevents the use of these steels developmenting. Recent investigations show that the cryogenic IGF of high manganese austenitic steels can be suppressed by the use of electroslag remelting (ESR)[3] and alloying with molybdenum and/or chromium.[4–6] The purpose of this paper is to report on the mechanical properties and the phase stability of ESR 32Mn-7Cr-0.6Mo-0.3N austenitic steel.

2. Experimental Procedure

The experimental steel was melted in a 120 kg inductive furnace, and then cast as electrodes for ESR. The chemical composition (wt.%) of the steel after ESR is of 0.098% C · 31.15% Mn · 7.34% Cr · 0.69% Mo · 0.30% N · 0.39% Si · 0.0194% P · 0.003% S, and the balance is iron.

The ESR ingot was hot rolled to plates of 24 and 12 mm in thickness. Two plates were austenitized at 1323 K for 1 h followed by quenching in ice-salt water and aging at 723 K for 45 min; they were then machined into mechanical test specimens. The dimension of the tensile specimen is 5 mm in diameter, and the Chappy impact specimen is 10 × 10 × 55 mm. Based on previous works, the plane strain fracture toughness K_{IC} of this steel is estimated at about 200 MPa $\cdot$ $m^{1/2}$, and the required thicknesses of the specimen are up to 200 mm. Therefore, it is difficult to measure the value of K_{IC} directly. Reducing the specimen thicknesses shifts the linear elastic properties to elastic plastic fracture mechanics. The

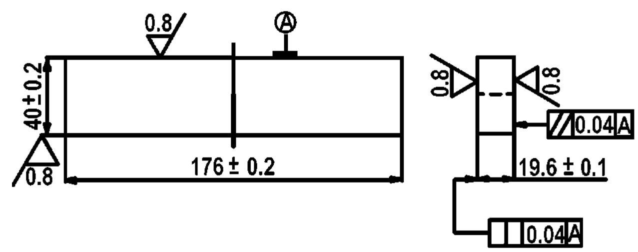

Fig. 1 Dimension of fracture toughness test specimen

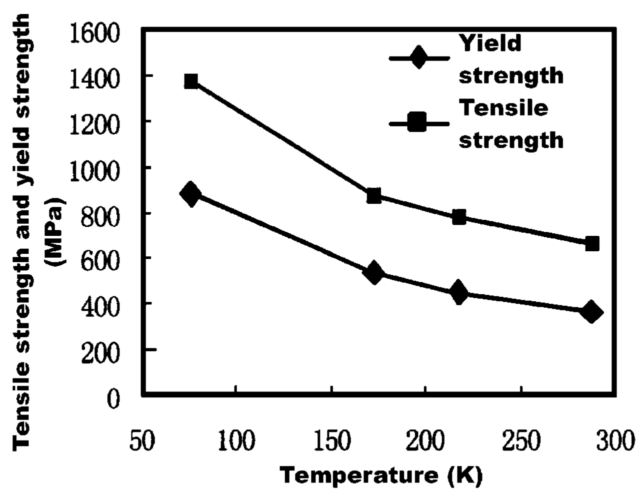

Fig. 2 Relations between tensile strength, yield strength, and temperature

Fu Ruidong, Zheng Yangzeng, and **Ren Yibin,** Materials Science and Engineering Department, YanShan University, Qinhuangdao, Hebei, 06604 China. Contact e-mail: furuidong001@yahoo.com.cn.

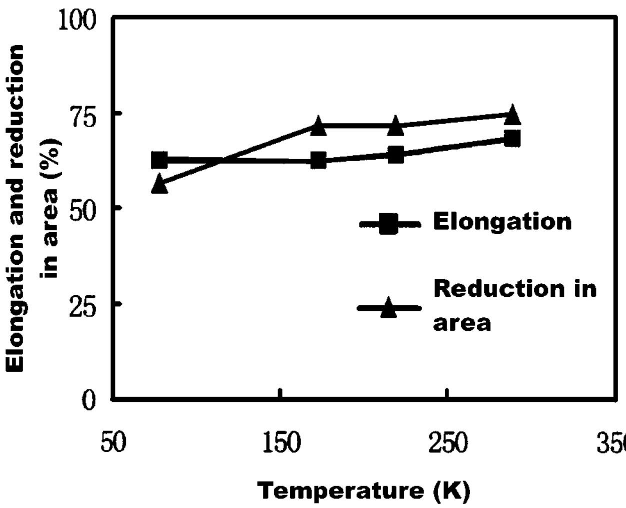

Fig. 3 Relations between elongation, reduction in area, and temperature

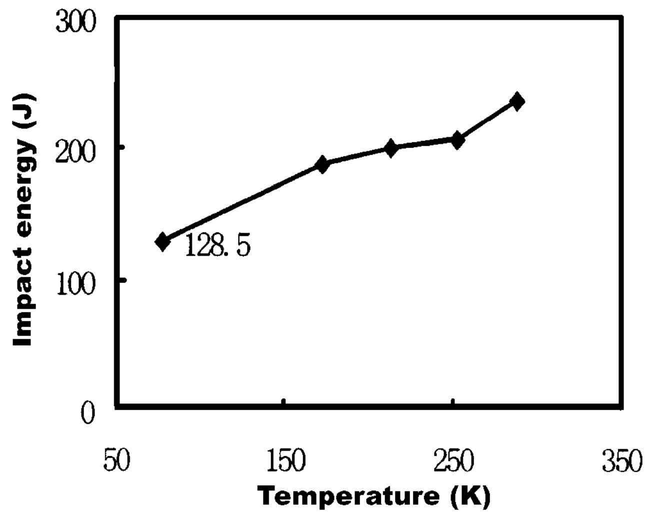

Fig. 5 Relations between impact energy and temperature

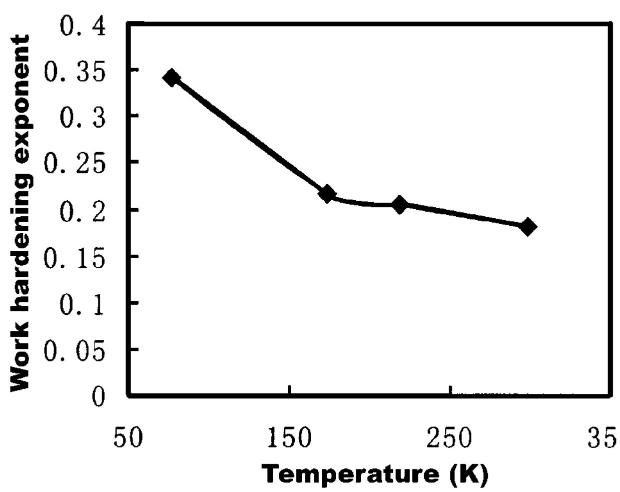

Fig. 4 Relations between work-hardening exponent and temperature

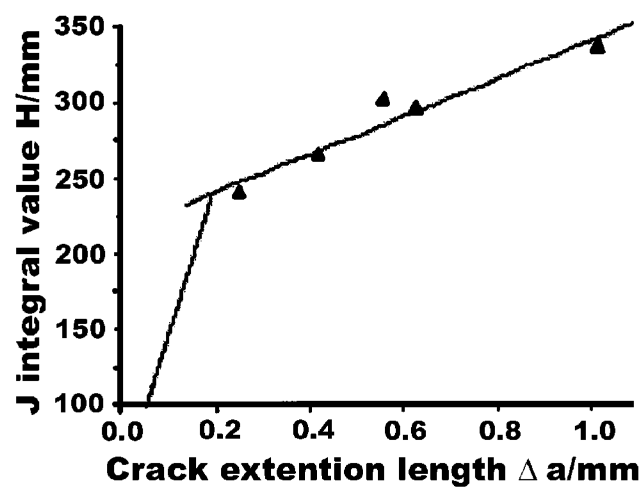

Fig. 6 J_R-Δa curve of this steel

Table 1 Test values of fracture toughness at 77 K

No.	*B* (mm)	*W* (mm)	*da* (mm)	*Ps* (KN)	*Je* (kJ/m²)	*Jp* (kJ/m²)	J_R (kJ/m²)
1	19.77	40.0	1.02	45.28	98.66988	232.9296	333.5995
2	19.68	39.88	0.63	48.72	104.7007	189.6203	294.3210
3	19.17	40.25	0.56	46.75	72.94987	227.2560	300.2059
4	19.74	40.08	0.42	49.21	104.9721	159.7182	264.6902
5	19.74	40.04	0.25	45.77	100.4313	138.4483	238.8797

application of the *J* integral is assumed to be valid in this case as a suitable method for performing K_{IC} measurements. Here, we employ $K_{J0.05}$ (condition fracture toughness) as the criterion. This value is converted from a $J_{0.05}$ value measured *via* the J_R-Δa chart (shown in Fig. 6; here, this is called the resistance curve method). Required specimen dimensions are shown in Fig. 1, and duplicate samples were prepared for each test condition. The fracture surfaces and the phase constitution of the deforming area at 77 K were investigated using scanning electron microscopy and x-ray diffraction, respectively.

3. Experimental Results and Analysis

3.1 Mechanical Properties

A series of tensile tests on 32Mn-7Cr-0.6Mo-0.3N austenitic steel show that, with a decrease in temperature, the tensile

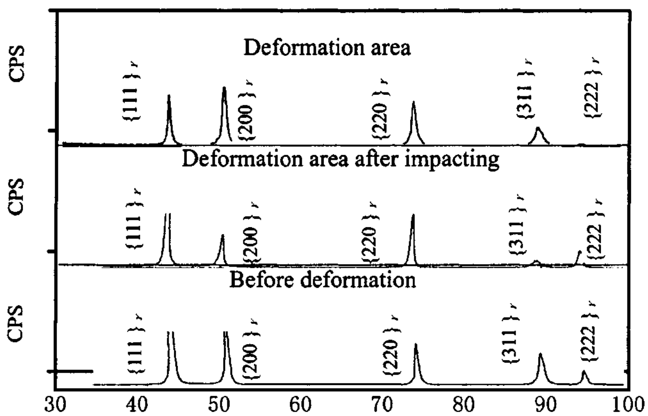

Fig. 7 The phase composition before and after deformation at 77 K

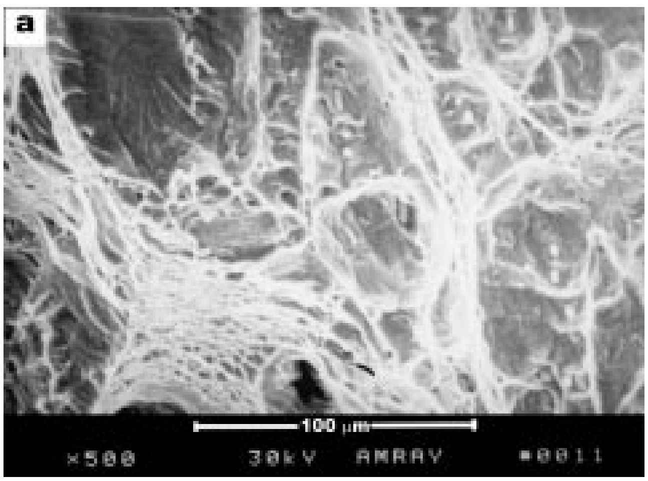

(**a**)

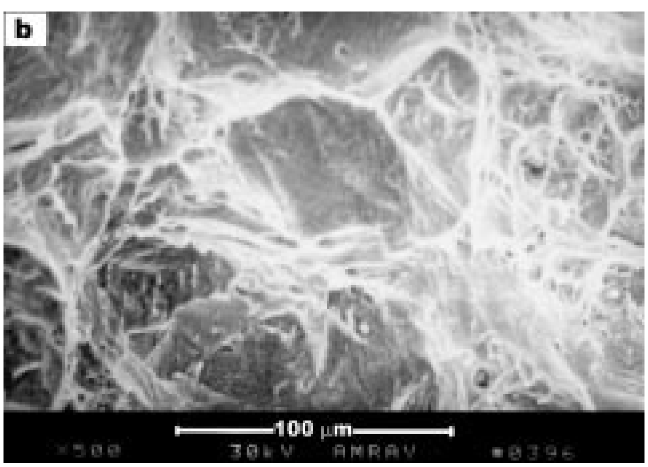

(**b**)

Fig. 8 77 K tensile and impact fracture suface: (a) tensile microsection and (b) impact microsection

strength (σ_b) and yield strength ($\sigma_{0.2}$) increase. The elongation (δ_5) does not change, but the reduction in area (ψ) slightly decreases (as shown in Fig. 2 and 3). The 77 K tensile properties

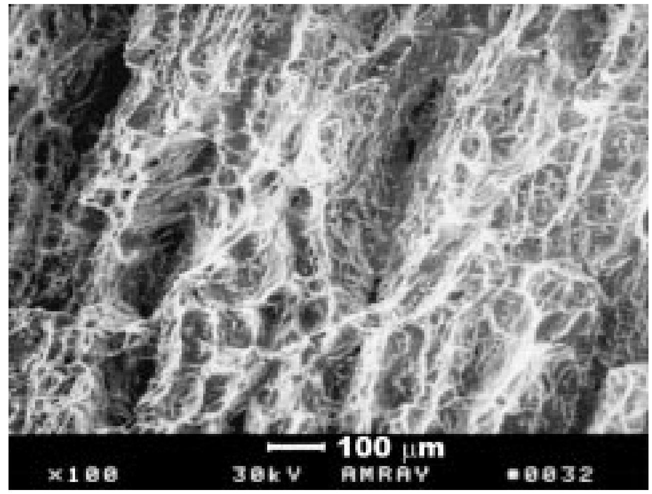

Fig. 9 Fracture surface of fracture toughness specimen at 77 K

are as follows: $\sigma_{0.2}$ = 883 MPa, σ_b = 1365 MPa, δ_5 = 62%, and ψ = 56.2%. The relations between the work-hardening exponent and temperature are shown in Fig. 4. The 77 K work-hardening exponent n is 0.34. The relationship between $\sigma_{0.2}$ and temperature is $\sigma_{0.2} \cdot 1392.4 \exp(-0.0106\ T) \cdot 300$.

The impact toughness results show that the impact energy decreases as the temperature decreases (as shown in Fig. 5), but the 77 K impact energy is still 128 J.

The 77 K data on the fracture toughness tests are shown in Table 1. According to these data, the J_R-Δa curve of this steel is drawn in Fig. 6. From the curve, the value of $J_{0.05}$ (which stands for the value of the J integral when crack extension length is 0.05 mm) can be demonstrated. Based on the equation $K_{J0.05} \cdot \sqrt{\frac{EJ_{0.05}}{1 - \nu^2}}$, the $K_{J0.05}$ value is 236 MPa · mm$^{1/2}$. Here, E = 206,000 MPa, and ν = 0.3.

3.2 Microstructure and Fracture Surface

From Fig. 7, it can be seen obviously that the phase composition of 32Mn-7Cr-0.6Mo-0.3N is single austenite before and after deformation, even at 77 K. The steel has a high microstructure stability.

The fracture surface of 77 K tensile and impact specimens is shown in Fig. 8(a) and (b). They all visibly exhibit a tough character composed of a huge quantity of dimples and a few quasi-cleavage facets. The fracture surface of 77 K fracture toughness test specimens also exhibits tough character (as shown in Fig. 9).

From the above results, it can be concluded that the cryogenic intergranular fracture of 32Mn-7Cr-0.6Mo-0.3N austenitic steel has been fully suppressed after ESR. Meanwhile, this steel exhibits an excellent cryogenic strength.

4. Conclusions

- The relationship between the yield strength and temperature for 32Mn-7Cr-0.6Mo-0.3N austenitic steel is as follows:

$\sigma_{0.2} \cdot 1392.4 \exp(-0.0106\ T) \cdot 300$. The 77 K yield strength is 883 MPa, and the $K_{J0.05}$ value is MPa $\cdot$ $m^{1/2}$.

- The cryogenic intergranular fracture is fully suppressed. The 77 K fracture surface exhibits a tough character composed of a huge quantity of dimples and a few quasi-cleavage facets.
- It can be hypothesized that the solid-solution strengthening of N atoms and the high cryogenic toughness are both due to the use of ESR and the addition of grain boundary toughening elements, such as Cr and Mo.

Acknowledgment

This work is sponsored by the China National Natural Science Foundation.

References

1. Koji Shibata and Yosuhike Kobiki: in *Mechanical Properties of High Yield Strength High Manganese Steels at Cryogenic Temperatures. Advances in Cryogenic Engineering Materials,* A.F. Clark and R.P. Reed, eds., Plenum Press, New York, NY, 1984, vol. 30, pp. 153-60.
2. R. Miura and H. Nakajima: in *Advances in Cryogenic Engineering Materials,* A.F. Clark and R.P. Reed, eds., Plenum Press, New York, NY, 1986, vol. 32, pp. 245-52.
3. Fu Ruidong, Zheng Yangzeng, and Li Shaohua: *J. Iron Steel Res.,* 2000, vol. 7 (1), pp. 31-35.
4. Zhang Jingwu, Zheng Yangzeng, and Liu Wenchang: *Cryogenic Eng.,* 1993, vol. 3, pp. 373-75 (in Chinese).
5. Xue Kanshi and Zhang Jingjiang: in *Advances in Cryogenic Engineering,* R.P. Reed, ed., Plenum Press, New York, NY, 1994, vol. 40, pp. 1275-81.
6. Xue Kanshi and Shun Dayong: *Chin. J. Mech. Eng.,* 1998, vol. 34 (6), pp. 11-15 (in Chinese).